PERGAMON

International Journal of Heat and Mass Transfer 45 (2002) 2729–2738

International Journal of HEAT and MASS TRANSFER

www.elsevier.com/locate/ijhmt

Characteristics of falling film flow on completely wetted horizontal tubes and the associated gas absorption

T. Nosoko [a,*], A. Miyara [b], T. Nagata [a]

[a] Department of Mechanical and Systems Engineering, University of the Ryukyus, Okinawa 903-0213, Japan
[b] Department of Mechanical and Systems Engineering, Saga University, Saga 840-8502, Japan

Received 5 June 2001; received in revised form 20 August 2001

Abstract

Falling water films on completely wetted horizontal tubes of 16 mm diameter in a vertical row and the associated oxygen gas absorption were experimentally investigated in the Reynolds number range of $10 < Re < 150$. It was found that the falling films form continuous sheets between the tubes when the tube spacing L_s is 2 mm, and that the film surfaces are smooth for $Re < 30$ whereas fine random waves appear on the surfaces for $Re > 30$. When $L_s = 5$ mm or larger, dripping from each tube occurs and causes the larger amplitude waves which rapidly spread on the film on the lower tube.

The Sherwood number, *Sh*, greatly increases with an increase in L_s from 2 to 5 mm and then levels off at $L_s = 10$ mm or larger. When $L_s = 2$ mm, *Sh* is in proportion to $Re^{1.15}$ for $Re < 30$ and to $Re^{0.9}$ for $Re > 30$. The *Sh* varies as $Re^{0.86}$ for the whole *Re* range at $L_s = 5$–15 mm. Comparison of the present results with empirical equations for vertical tube absorber indicates that volume of horizontal tube absorber can be smaller than that of vertical tube absorber by a factor of 1/1.18–1/2.2.

Keywords: Mass transfer; Gas absorption; Liquid film; Horizontal tube; Surface wave

1. Introduction

Heat and/or mass transfer across falling liquid films occurs in chemical and process engineering applications such as condensers, evaporators, gas absorbers, desorbers, and rectification equipment. Among various configurations of falling film flow, the falling films on the outside of horizontal smooth tubes have been widely employed when heat and mass transfer simultaneously occur across the films.

The flow between horizontal tubes in a vertical row as well as the film flow on the tubes shows distinct characteristics at different flow rates and spacings between tubes. These flow characteristics may highly affect the heat and mass transfer rates. Many investigations have been performed for the absorption of water vapor into falling films of aqueous lithium bromide (LiBr) solution on horizontal tube arrays. Cosenza and Vliet [1] performed experiments with a five-tube array of 18.8 mm diameter and found that introducing surfactant additive to the solution caused the complete wetting on the tubular surfaces and the Nusselt number *Nu* for the falling films increased from 1.19 to 2.25 in proportion with *Re* to a power of 0.46 for the range $2.5 < Re < 10$, indicating that the heat transfer coefficient *h* increased with *Re* to a power of 0.127. Their experimental data for *Nu* and overall vapor absorption rate were scattered widely by approximately 60% and 90% at maximum, respectively.

Kiyota et al. [2] employed the solution without surfactant additive which flows over 2–10-tube arrays of 28 mm diameter, and found that the data for heat and mass transfer coefficients across the films were in agreement with each other for 6–10-tube arrays and that the heat transfer coefficient *h* increased from 0.9 to 1.5 kW m^{-2} K^{-1} as *Re* to a power of approximate 0.2 for the range of flow rates $0.4 < Re < 5$ whereas the mass

* Corresponding author. Tel.: +81-98-895-8616; fax: +81-98-895-8616.
E-mail address: yongrang@tec.u-ryukyu.ac.jp (T. Nosoko).

0017-9310/02/$ - see front matter
PII: S0017-9310(01)00357-X

Nomenclature

A_w	wetted area of tubular surface (m^2)
C	constant
C_{in}	concentration of dissolved oxygen at entrance (kg m^{-3})
C_{out}	concentration of dissolved oxygen at exit (kg m^{-3})
C_{pc}	coefficient of compactness, Eq. (7)
C_s	saturated concentration of dissolved oxygen, Eq. (2) (kg m^{-3})
D	diffusivity (m^2 s^{-1})
g	acceleration due to gravity (m s^{-2})
h	heat transfer coefficient (W m^{-2} K^{-1})
k	mass transfer coefficient (m s^{-1})
L_p	distance between neighboring tubes in a vertical row (m)
L_w	distance between neighboring tube rows (m)
L_s	spacing between tubes (m)
N	number of tubes in single-column tube bank
n	constant
Nu	Nusselt number ($= h\delta/\lambda$)
P	ambient pressure (Pa)
p	vapor pressure of water (Pa)
R	radius of tube (m)
Re	Reynolds number ($= \Gamma/v$)
Sc	Schmidt number ($= v/D$)
Sh	Sherwood number ($= k\delta/D$)
T	temperature of film (K)

Greek symbols

α	solubility coefficient
Γ	half volumetric flow rate per unit tube length (m^2 s^{-1})
δ	Nusselt film thickness, Eq. (4) (m)
λ	thermal conductivity (W m^{-1} K^{-1})
v	kinematic viscosity (m^2 s^{-1})
ρ	density (kg m^{-3})

transfer coefficient k decreased from 3.0×10^{-6} to 2.2×10^{-6} m s^{-1} as Re to a power of approximately -0.12 for the same range of Re. The data were scattered by 20% and 30% for the heat and mass transfer coefficients, respectively. They assumed the complete wetting on the tubular surfaces when calculating both coefficients.

Furukawa et al. [3] found that k increased monotonously from 1.7×10^{-6} to 4.510^{-6} m s^{-1} with the flow rate of $LiBr/H_2O$ solution for the range 0.014 kg m^{-1} $s^{-1} < \rho\Gamma < 0.041$ kg m^{-1} s^{-1} (roughly corresponding to the range $4 < Re < 12$) without the surfactant additive and that introducing surfactant additive caused an increase in k that is 3.2–5.4 times what is measured at the same flow rate without the surfactant additive. They also assumed complete wetting when calculating the coefficient, and attributed the drastic increase in k to an increase in the wetted area A_w and Marangoni convection in the film caused by the surfactant additive.

Yamaguchi et al. [4] and Nomura et al. [5] measured A_w on a 13-tube array of 16 mm diameter and 5 mm tube spacing and used the measurements of A_w in the calculation of k. They found that the ratio of the wetted area was approximately 50% without the surfactant additive, and introducing the additive caused the complete wetting and the twofold increase in the overall absorption rate. They also showed that k rapidly increased from 6.5×10^{-5} to 12×10^{-5} m s^{-1} with $\rho\Gamma$ for the range 0.012 kg m^{-1} $s^{-1} < \rho\Gamma < 0.029$ kg m^{-1} s^{-1} (roughly corresponding to $1.8 < Re < 4.2$) and then practically leveled off at 0.029 kg m^{-1} $s^{-1} < \rho\Gamma < 0.053$ kg m^{-1} s^{-1} ($4.2 < Re < 7.7$). The heat transfer coefficient h had a gentle peak of 0.62 kW m^{-2} K^{-1} at $Re \approx 2.5$, and introducing the additive caused a very small increase in h. They did not attribute the drastic increase in the overall absorption rate to Marangoni convection but mainly to the increase in A_w caused by the additive.

Sideman et al. [6] investigated the mass transfer from the bulk of a falling film of aqueous sodium hydroxide solution to the interface between the film and the single horizontal tube, and measured the mass transfer coefficient k at various flow rates and spacings between the test tube and the upper tube. They observed that the solution flowed in the form of droplets, continuous jets, a continuous sheet or fragmented sheets between the tubes, and the droplet flow caused an increase in k that was approximately two times what was measured at the same flow rate when the continuous sheetwise flow occurred between tubes. Wassenaar [7] performed the absorption of water vapor into $LiBr/H_2O$ solution films on a 10-tube array of 12 mm diameter at various tube spacings and has found that there was no correlation between the flow behavior between tubes (droplet or jet) and the heat and mass transfer.

As reviewed above, there are large differences among the experimental results obtained by those researchers; Kiyota et al. showed the monotonous decrease in k with Re whereas the other researchers showed the increase in k, Nomura et al. found the gentle peak of h whereas the other researchers showed the monotonous increase in h with Re, and Sideman et al. claimed the large change in k with the flow behavior between tubes whereas Wassenaar did not. One of the main reasons for these

discrepancies may be the difficulty arising when determining the mean concentration difference between the surface and the bulk of the films and the mean temperature drops across the films that the gas is absorbed into. There is a large concentration gradient at the film surfaces because of the very small diffusivity. The equilibrium concentration and temperature at the surface are mutually related to each other and each one should be estimated by introducing some assumption to determine the other. This may cause large errors in determining the surface temperature and concentration, resulting in the discrepancies mentioned above. The appearance of dry patches on the tubes is another reason for those discrepancies. The wettability on the tube surfaces is very sensitive to a trace of impurities as well as the interfacial properties of the tubes and the films, and therefore the rate of wetted area on the tubes may vary with the experiments by different workers. The appearance of dry patches causes a decrease in the film surface area where gas absorption occurs. Most workers did not, however, determine the wetted area on the tubes and calculated the mass transfer coefficient k assuming the complete wetting.

Many theoretical models [2,7–10] have been presented to predict the heat and mass transfer rates across the falling films, and for simplification these models introduced the assumptions: (a) the films have smooth surfaces and the flow is laminar, and (b) the flow behavior between tubes can be theoretically described only as the cause of the complete mixing or no mixing. As shown later in Section 3, the first assumption is not valid under the conditions for practical use, and therefore these models may provide erroneous predictions.

In this work, we achieved the complete wetting of falling water films on copper tubes without any additives and performed the oxygen gas absorption into the films on horizontal smooth tubes at various tube spacings and flow rates. The heat of absorption of oxygen is small enough to assume isothermal films and the concentration at the film surfaces is accurately determined from the temperature of the isothermal films, resulting in a high accuracy in the measurements of k. We also observed the flow on the tubes and between tubes, and discussed how the flow characteristics affect the mass transfer.

2. Experimental apparatus and procedure

2.1. Experimental apparatus

An illustration of the experimental apparatus used in this investigation is presented in Fig. 1. The horizontal tube assembly is placed in the rectangular casing which is equipped with the front and back glass plate windows. The assembly consists of the single-column copper tube

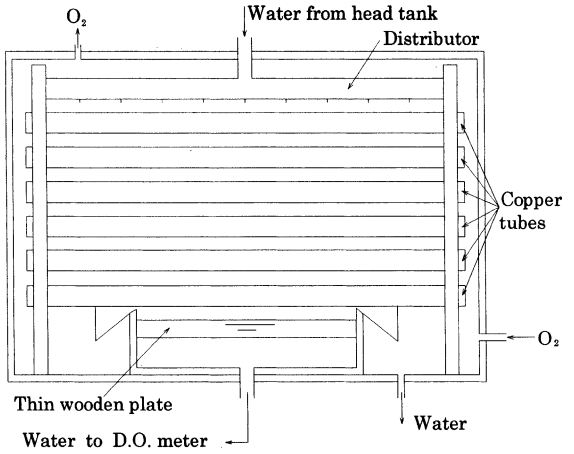

Fig. 1. Schematic diagram of the gas absorption apparatus.

bank of 16 mm diameter and 284 mm wetted length, the distributor introducing water onto the tubes and the gutter collecting oxygen rich water from the bottom tube. Various tube assemblies were tested: 2-, 4-, 6- and 8-tube arrays with 2, 5, 10 and 15 mm tube spacings.

The distributor has stainless steel capillary tubes of 1.5 mm inner diameter and 8 mm length at intervals of 15 or 30 mm, through which tap water is fed onto the tubes. The flow rates through these capillary tubes were in good agreement with each other within ±2%.

The inside of the gutter is 6 mm wide, 120 mm long and 42 mm high. The 2 mm thick wooden plate is attached to the bottom tube so that water flows from the tube into the water pool in the gutter in the form of falling films on the wooden plate. The film flow and the small water surface of the pool may minimize the extra gas absorption in the gutter. The gutter is placed at the center to collect the water flowing over the center part of the tubes where the effects of the side walls are negligibly small.

2.2. Procedure

Oxygen gas started 1 h before experimental runs to flow continuously into the casing through the hole at the bottom of a side wall and then flows out through the hole in the top wall. The flow rates of oxygen gas were small enough to assume that the pressure in the casing is equal to the ambient pressure P. Tap water from an overflowing head tank (not shown in Fig. 1) flows into the distributor and then onto the copper tubes at a constant flow rate. Oxygen rich water from the gutter flows into the small container (not shown in Fig. 1) in which the water was stirred by a magnetic stirrer and the dissolved oxygen concentration C_{out} was measured within ±1% error with a probe and an ammeter, model OE-2101 and DO-25A, made by Toa-Denpa. The flow

rate from the container was measured with a stopwatch and an electrical balance, and the water temperature T was measured at the bottom of the casing with a T-type thermocouple.

Just before and after a series of experimental runs in a day, tap water was directly introduced into the small container to measure the dissolved oxygen concentration. The average of both measurements was employed as the concentration C_{in} of water entering the apparatus. Before a series of experimental runs in a day, all the copper tubes in the array were polished with emery paper of #500 to achieve the complete wetting. When taking pictures of falling films on the tubes with a digital camera and a flash tube, the front and back windows were removed from the casing and a black surface board was placed behind the apparatus.

2.3. Equation for the determination of mass transfer coefficient and dimensionless groups

Introducing the overall log–mean concentration difference, the mean mass transfer coefficient k is defined as

$$k = \frac{\Gamma}{\pi R N} \ln \frac{C_s - C_{in}}{C_s - C_{out}}. \tag{1}$$

The water at the film surface is in equilibrium with the partial pressure of oxygen gas, and therefore the concentration C_s at the film surface may be expressed by Henry's law as

$$C_s = \frac{32.0}{22.4} \alpha \frac{P - p(T)}{1.013 \times 10^5}, \tag{2}$$

where the saturated vapor pressure of water $p(T)$ is a function of the surface temperature T (= the isothermal film temperature) and available from the data book [11].

The Sherwood number Sh is defined in terms of the Nusselt film thickness δ as

$$Sh = \frac{k\delta}{D}, \tag{3}$$

$$\delta = \left(\frac{3\nu\Gamma}{g} \right)^{1/3}, \tag{4}$$

where δ is the thickness of laminar film falling down a vertical surface and Eq. (4) may represent the film thickness at 90° from the top of the horizontal tubes.

The Reynolds number Re is defined as

$$Re = \frac{\Gamma}{\nu}. \tag{5}$$

The measurements of different workers have showed that Sh increases with Schmidt number Sc to 0.5 power for gas absorption or desorption of liquid film falling down vertical surfaces [12,13], and we assume that it is valid for the falling films on the horizontal tubes. The surface tension of the films also is another physical property that may affect the flow behavior and the mass transfer. We only employed water as the test liquid and performed the experiments for a narrow range of film temperatures ($T = 18$–23) or surface tension (7.2×10^{-2}–7.3×10^{-2} N m^{-1}), and therefore the effects of surface tension have not been discussed in this paper.

3. Results and discussion

3.1. Observations of the flow over tubes and between tubes

The film flow behavior at various tube spacings L_s and Reynolds numbers Re is shown in Fig. 2. The sheetwise flow occurs between tubes at $L_s = 2$ mm. The film surfaces on tubes are observed to be smooth for the range of $Re < 30$ (see Fig. 2(a)) whereas they show roughness, i.e. the occurrence of fine random waves, and the random wave motion become vigorous with increasing Re for $Re > 30$ (Fig. 2(b)).

At $L_s = 5$ mm or larger, the continuous sheetwise flow breakup and discontinuous "droplet flow" are observed between tubes. Droplets are hanging on the bottom of each tube at some intervals and even grow to be large enough to touch the film on the lower tube. This touching causes the vigorous changes in a moment: A part of a hanging droplet is absorbed into the film, causing waves rapidly spreading on the film and the breakup of the hanging droplet into the absorbed part and the residue which is retracting quickly to the bottom of the upper tube. The spreading waves have a larger amplitude than that of the fine random waves which appear at $L_s = 2$ mm. The distances of the dripping sites on the top tube are close to the interval of the capillary tubes of the distributor, and become random as it goes to the lower tubes: the droplets fall from random dripping sites at random time intervals. On average, the distances between the dripping sites are larger on the lower tubes since the random distances cause some neighboring sites with small spacings to merge as it goes to the lower tubes. The dripping sites and the time intervals become more random, and the distances between the sites increase and the time intervals decrease with increasing Re.

At $L_s = 5$ mm the hanging droplets grow into half spheres and then touch the films on the lower tube causing the waves to spread on the films (Fig. 2(c)). The merging of droplet sites causes a droplet of irregular shape or a "lump" with larger volume. The lumps touching the film on the lower tube also cause the waves spreading on the film (see the lower tubes in Fig. 2(d)).

The hanging droplets grow into "columns" which touch the film on the lower tube at $L_s = 10$ mm (Fig. 2(e) and (f)). The columns break up and the residues retract completely to the bottom of the upper tube at low flow rates (Fig. 2(e)) whereas the retraction is not complete at higher flow rates, and finally they become the "quasi-

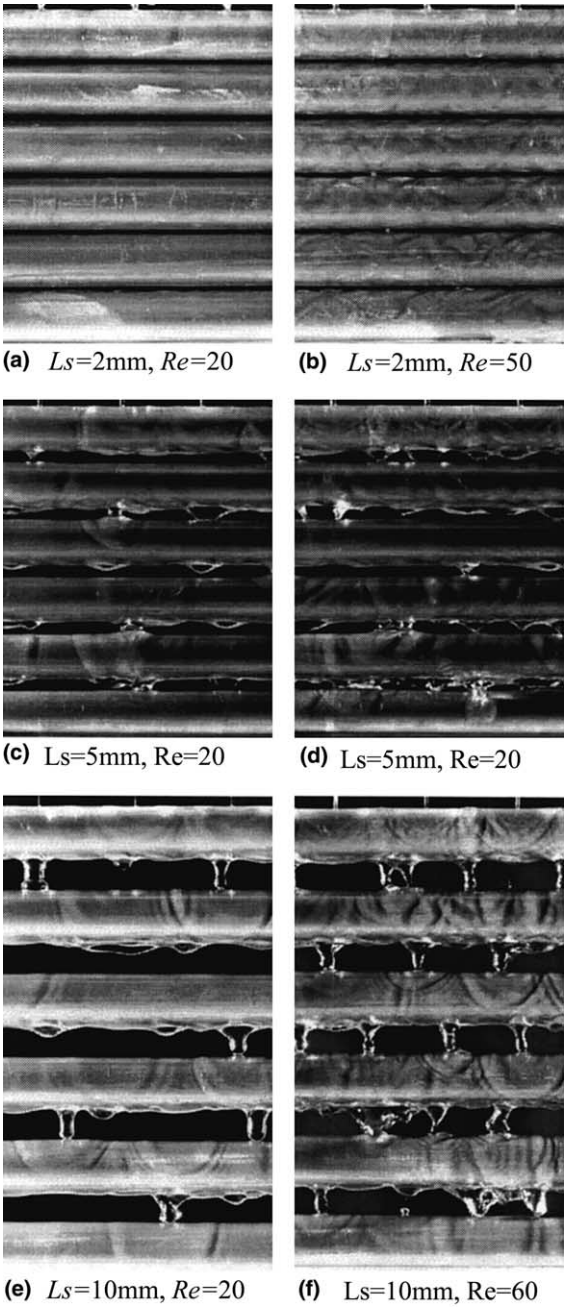

Fig. 2. Flow behaviors between tubes and falling films on the tubes.

steady column'' (Fig. 2(f)). The quasi-steady columns might give the appearance of a continuous jet flow in the still photograph in Fig. 2(f), but the bottom surfaces of the columns are repeatedly touching the film on the lower tube at high frequencies, causing the waves to rapidly spread on the film. This flow behavior is discontinuous and should be categorized into the droplet flow. The water lumps are observed on the lower tubes (Fig. 2(f)), which also cause the waves spreading on the films.

At $L_s = 15$ mm, the columns are also formed between tubes, which are longer than those at $L_s = 10$ mm. The 15 mm spacing is not large enough that the columns break up to produce isolated droplets before touching the film on the lower tube. The flow behavior of the films and between tubes is basically similar to that observed at $L_s = 10$ mm, but the waves spreading on films are more intense because of the larger volume of water absorbed at each touching.

The droplet flow and continuous sheetwise flow are only observed between tubes in the present experiments whereas Sideman et al. [6] observed the other kinds of flow behavior, i.e. fragmented sheets when $L_s = 4$ and 6 mm and $Re \approx 160$ or smaller and jets between tubes when $L_s = 10$ mm or larger and $Re \approx 160$ or larger. The liquid they used has a surface tension of 1.0×10^{-2} N m^{-1} and a density of 1.1×10^3 kg m^{-3}. The surface tension of the liquid is much smaller than that of water (7.2×10^{-2} N m^{-1}) and this may be the main reason why the jets and the fragmented sheets were observed in their experiments. The jets and the fragmented sheets are much more unstable for high surface tension liquid such as water, and they might occur under very limited conditions for water. Moreover, they observed that the small surface tension liquid produced isolated droplets after the breakup of the liquid columns hanging on the tube at $L_s = 10$ mm or larger.

3.2. Total volume of droplets jumping off tubes

It was observed that droplets are jumping off the tube array when the Reynolds number and the tube spacing L_s are large. We collected the droplets jumping off the center part of the tubes using a 120 mm long ''dustpan'' and then measured the total volume of the collected water at various Re and L_s for the 2–8-tube arrays. Fig. 3 shows the variations of volumetric ratio of the collected droplets to the water fed onto the tubes with tube spacing L_s at a constant $Re \approx 78$. The total volume of the droplets jumping off the tubes is negligibly small for the 2–6-tube arrays with 5 mm tube spacing whereas it is much larger for the 6-tube array with 10 and 15 mm tube spacings.

Fig. 4 shows the total volume of droplets increasing with Re for 2–8-tube arrays at a constant tube spacing of $L_s = 10$ mm. The total volume of the droplets is less than 4% of the feeding water for 2- and 4-tube arrays whereas it increases exponentially with increasing Re up to 19% and 26% at $Re \approx 91$ for 6- and 8-tube arrays, respectively.

The flow rates of films decrease as it goes to the lower tubes because of the droplets jumping off the tubes, and we use the Reynolds number Re defined in terms of the flow rate Γ leaving the bottom tube in this paper. The

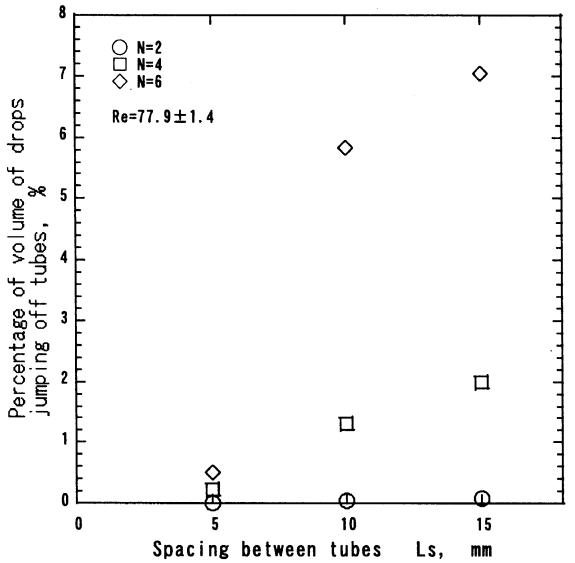

Fig. 3. Tube spacing and variation of volumetric percentage of droplets jumping off tubes.

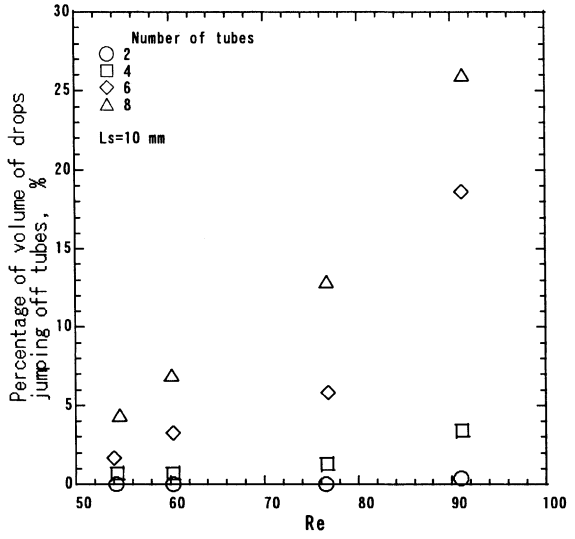

Fig. 4. Reynolds number *Re* and variation of volumetric percentage of droplets jumping off tubes.

decrease in the flow rate is small (by approximately 6% or less) for the ranges of *Re*, L_s and *N* where the mass transfer experiments were performed.

3.3. Effects of intervals between capillary tubes of the distributor on gas absorption

We employed two distributors with 15 and 30 mm distances between capillary tubes through which water was fed onto the copper tubes. Fig. 5 shows the increase

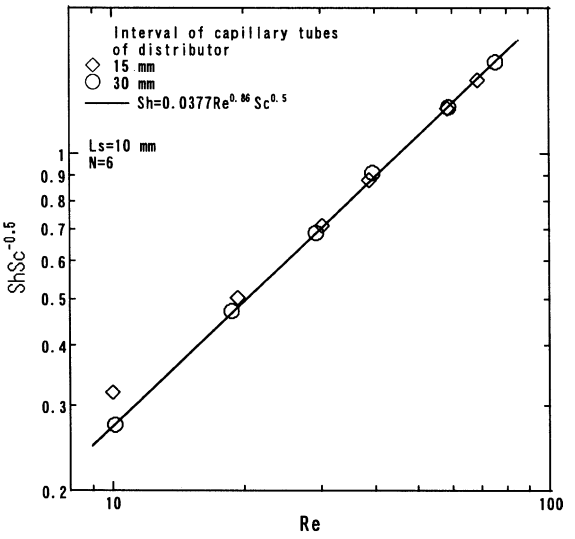

Fig. 5. Variation of Sherwood number *Sh* with Reynolds number *Re* at 15 or 30 mm distances between capillary tubes of distributor.

in *Sh* with increasing *Re* for 6-tube array with 10 mm spacing between copper tubes. The *Sh* increases as *Re* to a power of 0.86 when the distances between capillary tubes are 30 mm. The values for *Sh* obtained with the 15 mm distance capillary tubes are in good agreement with those with the 30 mm distance capillary tubes in the range $20 < Re < 80$, and the value for *Sh* with the 15 mm distance tubes is larger when $Re \approx 10$. It was observed that the 30 mm distance capillary tubes produced water jets over the whole *Re* range investigated whereas the 15 mm distance capillary tubes produced droplets falling onto the copper tubes at $Re \approx 10$ and jets for $Re > 20$. The droplet flow may cause more intense disturbances in the films on the copper tubes to enhance the gas absorption than the jet flow.

The 15 mm distance capillary tubes cause more number of dripping sites or "columns" on the bottom of the top copper tube than the 30 mm distance capillary tubes, and the number of dripping sites or columns more rapidly decreases as it goes to the lower tubes. This decrease is gentler for the 30 mm distance capillary tubes. The 30 mm distance is close to the one-dimensional "Taylor wavelength" (≈29.9 mm) of the wave that grows fastest during the collapse of an infinite plane horizontal interface between the upper heavy water and the lower light air [14]. Hereafter, the results obtained with the 30 mm distance capillary tube distributor will be discussed.

3.4. Effects of the number of tubes on gas absorption

Fig. 6 shows the variations of *Sh* with *Re* for the 2–8-tube arrays at a tube spacing $L_s = 10$ mm. The 6-tube

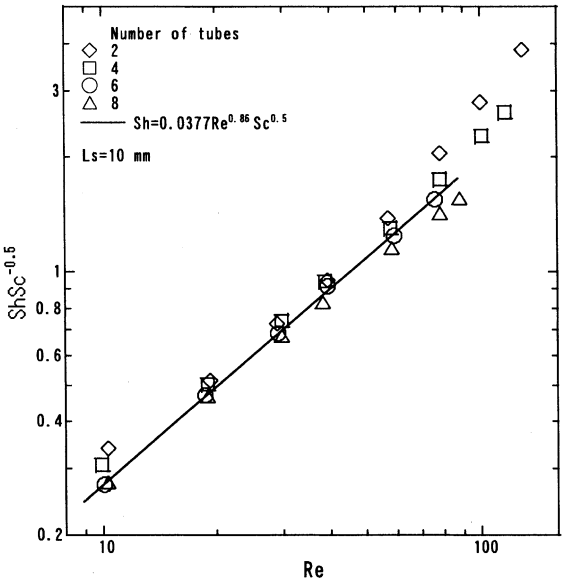

Fig. 6. Variation of Sherwood number *Sh* with Reynolds number *Re* at various number of tubes.

array shows the linear increase in $\log Sh$ with $\log Re$ which can be described by the power law correlation:

$$Sh = 0.0377Re^{0.86}Sc^{0.5}. \quad (6)$$

The 2-, 4- and 8-tube arrays show the similar increase in *Sh* to the 6-tube array, and the values for *Sh* are larger for the smaller number of tubes in the array. The difference in *Sh* is very small (less than 14%) in the range $20 < Re < 50$ for these tube arrays whereas it is about 24% at $Re \approx 10$ and increases with *Re* in the range $Re > 50$.

When calculating k by Eq. (1), it has been assumed that the area of the gas-absorbing water surface is equal to the total area of the tube surfaces. Hence the effects of the extra gas absorption in the gutter are larger for tube arrays of smaller number N of tubes, resulting in the larger *Sh*. The effects of the extra absorption decrease with increasing tube number N, and the difference in *Sh* between the 6- and 8-tube arrays is small (less than 13%) for the whole experimental range of $10 < Re < 90$. Hereafter the results obtained for the 6-tube arrays will be discussed.

3.5. Effects of tube spacing on gas absorption

Four different tube spacings, $L_s = 2$, 5, 10 and 15 mm, were tested at various flow rates using a 6-tube array. The variations of *Sh* with L_s at three Reynolds numbers are presented in Fig. 7. The *Sh* shows great increase with an increase in the tube spacing L_s from 2 to 5 mm for any Reynolds numbers whereas it shows a small increase in the range $L_s > 5$ mm and tends to

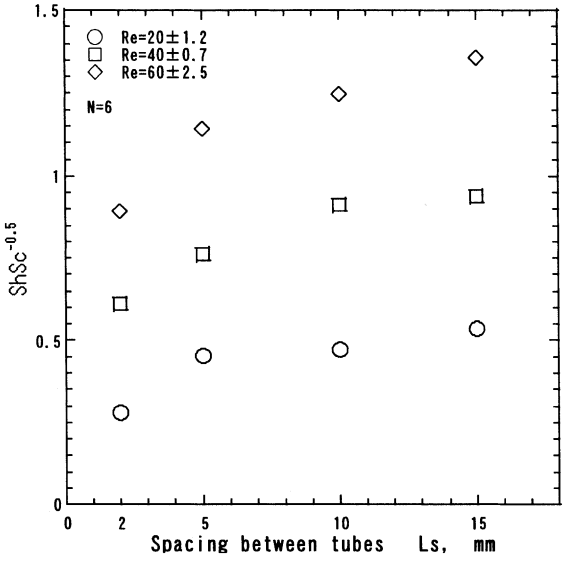

Fig. 7. Variation of Sherwood number *Sh* with tube spacing.

saturate for $L_s \geqslant 10$ mm. Fig. 8 shows the variations of *Sh* with *Re* for a 6-tube array of various tube spacings, comparing with Bakopoulos' equations [12] for gas absorption into a liquid film falling down a vertical surface. Bakopoulos' equations fit the experimental data by the other researchers [15–17] within +17% to −6% for the range $12 < Re < 70$ and ±24% for $70 < Re < 400$.

The 15 mm spacing tube array shows that the values for *Sh* are in good agreement with the values obtained with the 10 mm spacing tube array, and the 5 mm

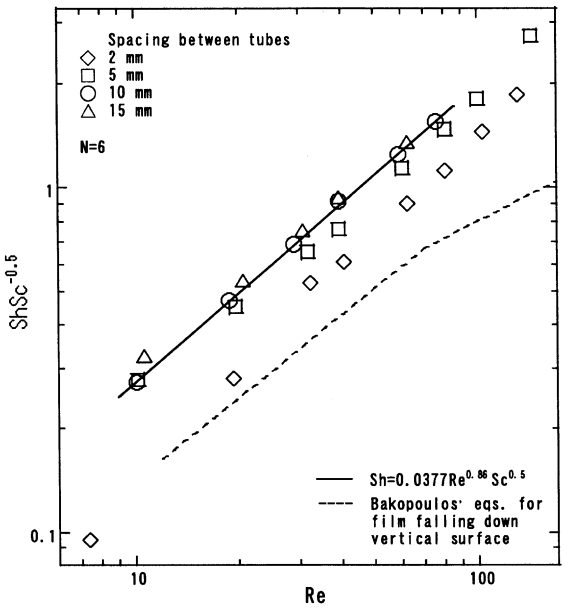

Fig. 8. Variation of Sherwood number *Sh* with Reynolds number *Re* at various tube spacing.

spacing tube array shows slightly lower values for *Sh* than the 10 and 15 mm spacing tube arrays. The differences in *Sh* are small and less than 20% for the whole *Re* range investigated.

For the 2 mm spacing tube array, *Sh* increases in proportion to *Re* to a power of 1.15 in the range $Re < 30$ and to a power of 0.9 in $Re > 30$, and the values for *Sh* are much smaller than those obtained with the other spacing tube arrays in the whole experimental *Re* range. As described in Section 3.1, the falling films on the tubes have smooth surfaces in $Re < 30$ whereas the surfaces show roughness (or fine random waves on them) in $Re > 30$ for the 2 mm spacing tube array. The 2 mm spacing tube array shows a similar increase in *Sh* to the 5–15 mm spacing tube arrays in the range $Re > 30$, but the values for *Sh* are smaller by approximately 30% or more for the 2 mm spacing array than the 5 mm or larger spacing arrays in $Re > 30$. These larger *Sh* values for 5–10 mm tube spacings are attributed to the discontinuous droplet flow between tubes that causes surface waves rapidly spreading on the films flowing over the tubes and the vigorous motion of the hanging droplets when they break up at 5 mm or larger spacing. It can be concluded that the discontinuous droplet flow between tubes enhances the absorption more than the continuous sheetwise flow, and that the flow behavior strongly affects the mass transfer, and changes values for *Sh* and moreover the power *n* in the power-law correlation $Sh = CRe^n$.

The present results are qualitatively consistent with the findings of Sideman et al. [6], i.e. the discontinuous droplet flow between tubes enhances the mass transfer at the interface between the tube and the film on it. Quantitatively the droplet flow causes a much more increase in the mass transfer coefficient at the film–wall interface than the free surface of the film. Sideman et al. found that the instantaneous mass transfer coefficient periodically varies with time at a frequency which is roughly equal to the frequency of dripping from the upper tube, and the droplet flow causes an increase in the transfer coefficient at the interface that is roughly two times what is measured when the continuous sheetwise flow occurs between tubes for the range $25 < Re < 150$. They concluded that the droplets fall onto the film and then penetrate into the film deep enough to affect the mass transfer at the tube wall.

As shown in Fig. 8, the droplet flow between tubes causes an increase in the mass transfer coefficient at the free surfaces of the films by 30–45% for the range $30 < Re < 150$. The fine random waves occur on the films with the sheetwise flow between tubes and may cause a large increase in the mass transfer coefficient at the free surfaces of the films. Hence the droplet flow between tubes superimposes the 30–45% increase in *k* which is smaller than the increase in the transfer coefficient at the tube wall.

As shown in Fig. 8, *Sh* increases in proportion to *Re* (or flow rate Γ) to a power of approximately 0.86 for the 5–15 mm spacing tube arrays in the whole *Re* range of the present work, and a power of 1.15 for the 2 mm spacing tube array in $Re < 30$ and 0.9 in $Re > 30$, respectively. This means that the mass transfer coefficient *k* increases as *Re* (or Γ) to a power of 0.53 for the 5–15 mm spacings, 0.82 for the 2 mm spacing in $Re < 30$ and 0.67 for the 2 mm spacing in $Re > 30$, since the film thickness δ is in proportion to *Re* (or Γ) to a power of 1/3 as shown in Eq. (4). Plotting the measurements of the other workers [3,4] in logarithmic graphs shows that *k* varies as $\rho\Gamma$ to a power of 0.4 and 0.83 for the measurements of Furukawa et al. [3] when $LiBr/H_2O$ solution film contains a surfactant additive and when it does not, respectively, and that the measurements of Yamaguchi [4] do not show a power law correlation between *k* and $\rho\Gamma$, but an initial rapid increase in *k* with $\rho\Gamma$ and then saturation of *k* at larger values for $\rho\Gamma$. The measurements of Kiyota et al. [2] show that *k* varies as *Re* to a power of approximately −0.12. Our measurements at $L_s = 5$–15 mm are roughly consistent with the results of Furukawa et al. when they used $LiBr/H_2O$ solution containing a surfactant additive to achieve the complete wetting of films on tubes.

Bakopoulos' equations show that *Sh* increases as *Re* to a power of 0.8 in the range $12 < Re < 70$ and to a power of 0.5 in $70 < Re < 400$ for a film falling down a vertical surface. The surface of the film is not smooth even at the small value $Re = 12$ and shows wavy motion or "rippling" [18,19]. The *Sh* is larger for the continuous film flow over the 2 mm spacing tubes with the sheetwise flow between tubes than Bakopoulos' equations for the range $Re > 12$, and the difference in *Sh* increases with *Re*. The film flow accelerates from the top of the horizontal tubes to the middle and then decelerates to the bottom, and therefore "the time of exposure" [20] of the film surface to oxygen gas is longer when the film flows on a horizontal tube from the top to the bottom than when it flows the same distance down a vertical surface. Mixing may occur in the sheets between the tubes, which is similar to the one occurring in the junctions between spheres. Ratclift and Reid [21] visualized the flow of a liquid film over a vertical "string" of touching spheres using a dye trace technique and observed mixing in the junctions between spheres. Davidson et al. [22] measured the carbon dioxide absorption rate into a water film flowing over spheres and found that complete mixing occurs at the junctions and drastically enhances the absorption. The results in Fig. 8 indicate that the mixing in the sheets between tubes and the longer exposure time of the films on tubes cause a great enhancement of gas absorption, and those effects on the absorption are larger than the effects of waves on the film falling down a vertical surface.

3.6. Compactness of absorber

When designing an absorber, compactness is one of the important factors to be concerned, and absorbers with a staggered arrangement of tubes can be more compact than those with a checkerboard arrangement. Assuming that the film surface area is equal to the tubular surface area, here we introduce the coefficient of compactness C_{pc} defined as

$$C_{pc} = \left(\frac{2\pi R}{L_p L_w}\right) \Big/ \left(\frac{2\pi R}{L_p L_w}\right)_{L_s=5\ \mathrm{mm}}, \tag{7}$$

where L_p and L_w are shown in Fig. 9, and 5 mm spacing is employed between a tube in a vertical row and a tube in a neighboring row. The 5 mm or larger spacing may be required so that a liquid bridge is not formed between tubes in neighboring rows. The coefficient C_{pc} represents the ratio of the tube surface area in unit volume of absorber with an arbitrary value for L_s to that with $L_s = 5$ mm.

Fig. 10 shows the variations in the multiple of Sh and C_{pc} with Re at various L_s values, comparing with Bakopoulos' equations for gas absorption into a liquid film falling down a vertical surface. Bakopoulos' equations in Fig. 10 represent the multiple of Sh and C_{pc} for a vertical tube bundle in a staggered arrangement with 5 mm tube spacing, where $C_{pc} = 1$ and the liquid films fall down the outer surfaces of the vertical tubes of 16 mm outer diameter.

The plots for $L_s = 5$, 10 and 15 mm are very close to each other, and can be fit by the equation

$$Sh\,C_{pc} = 0.035 Re^{0.86} Sc^{0.5}. \tag{8}$$

The coefficient C_{pc} decreases with increasing L_s whereas the mass transfer coefficient k increases (see Fig. 8), and there is the trade-off between them.

The multiple of Sh and C_{pc} is smaller by 10–20% for 2 mm tube spacing than the larger tube spacing in $Re > 30$, and the difference increases with decreasing Re in $Re < 30$. The increase in C_{pc} cannot make up the large decrease in Sh for 2 mm tube spacing.

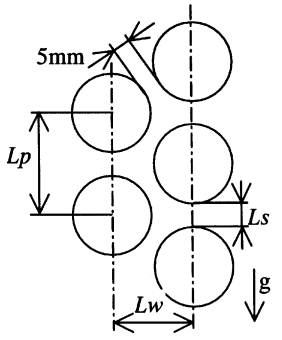

Fig. 9. Tubes in a staggered arrangement.

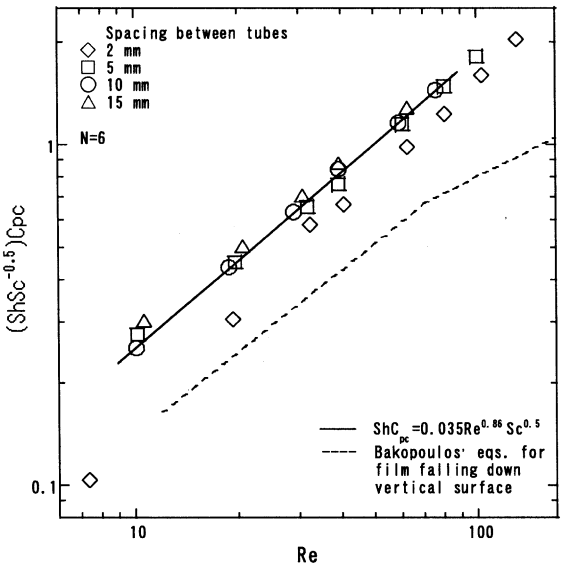

Fig. 10. Reynolds number Re and variation of the multiple of Sherwood number Sh and coefficient of compactness C_{pc}.

The comparison with Bakopoulos' equations shows that the multiple of Sh and C_{pc} for the horizontal tube bundles with 5–15 mm tube spacings is 1.8–2.2 times what is predicted by Bakopoulos' equations for the vertical tube bundle with 5 mm tube spacing, indicating that horizontal tube absorbers are much more compact than vertical tube absorbers. The volume of the former can be designed to be smaller than that of the latter by a factor of 1/1.8–1/2.2 when the same absorption rate is required to occur in both absorbers in which all tubes are completely wetted.

4. Conclusions

Falling water films on completely wetted horizontal tubes of 16 mm diameter in a vertical row are found to form continuous sheets between tubes when the spacing L_s between tubes is 2 mm, and the films are observed to have smooth surfaces for $Re < 30$ whereas fine random waves appear on the films for $Re > 30$. Dripping from the bottom of each tube occurs when $L_s = 5$ mm or larger, causing waves rapidly spreading on the film on the lower tube.

The total volume of droplets jumping off the 6-tube array is negligibly small at $L_s = 5$ mm or smaller but it increases exponentially with Re up to 20% or larger of the feeding water when $L_s = 10$ mm or larger.

The Sherwood number Sh greatly increases with an increase in L_s from 2 to 5 mm, an increase in L_s from 5 to 10 mm causes a small increase in Sh (by 20%), and Sh levels off for $L_s > 10$ mm. The Sh is in proportion to Re

to a power of 1.15 for the 2 mm spacing tube array when $Re < 30$ whereas a power of 0.9 when $Re > 30$. The 5–15 mm spacing tube arrays show that Sh varies as Re to a power of 0.86 for the whole Re range ($10 < Re <$ 80–150) of the present work, and the data for Sh obtained with the 10 and 15 mm spacing tube arrays may be described as a function of Re by Eq. (6).

Introducing the compactness coefficient C_{pc} defined by Eq. (7) for an absorber with a staggered arrangement of a tube bundle, it is shown that Eq. (8) fits the data for the multiple of Sh and C_{pc} obtained with 5, 10 and 15 mm spacing tube arrays. Comparison of Eq. (8) with Bakopoulos' equations indicates that horizontal tube absorbers with staggered tube arrangements can be smaller in volume than vertical tube absorbers by a factor of 1/1.8–1/2.2.

Acknowledgements

The authors gratefully acknowledge Mr. T. Hayashi and Mr. K. Oku for their assistance in this experiment. This work was supported by Tokyo Electric Power Co. Research Foundation.

References

[1] F. Cosenza, G.C. Vliet, Absorption in falling water/LiBr films on horizontal tubes, ASHRAE Trans. 96 (1990) 693–701.

[2] M. Kiyota, I. Morioka, Y. Sano, Steam absorption into films of aqueous solution of LiBr falling over multiple horizontal pipes, in: Proceedings of 35th Japan Heat Transfer Symposium, 1998, pp. 849–850.

[3] M. Furukawa, N. Sasaki, T. Kaneko, T. Nosetani, Enhanced heat transfer tubes for absorber of absorption chiller/heater, Trans. Jpn. Assoc. Refrig. 10 (1993) 219–226.

[4] S. Yamaguchi, N. Nishimura, Y. Nomura, R. Kawakami, Analysis of absorption and heat exchange performance of absorber of absorption chiller (2nd report: Discussion on wetted area with visualization), in: Proceedings of Japan Association of Refrigeration Meeting in 1993, pp. 129–132.

[5] Y. Nomura, N. Nishimura, H. Iyota, H. Kamiyo, K. Mori, Analysis of absorption and heat exchange performance of absorber of absorption chiller (Evaluation of local heat transfer with surfactant additive), in: Proceedings of Japan Association of Refrigeration Meeting in 1995, 1995, pp. 37–40.

[6] S. Sideman, H. Horn, D. Moalem, Transport characteristics of films flowing over horizontal smooth tubes, Int. J. Heat Mass Transfer 21 (1978) 285–294.

[7] R.H. Wassenaar, Measured and predicted effect of flowrate and tube spacing on horizontal tube absorber performance, Int. J. Refrig. 19 (1996) 347–355.

[8] G. Grossman, Simultaneous heat and mass transfer in film absorption under laminar flow, Int. J. Heat Mass Transfer 26 (1983) 357–371.

[9] B.J.C. van der Wekken, R.H. Wassenaar, Simultaneous heat and mass transfer accompanying absorption in laminar flow over cooled wall, Int. J. Refrig. 11 (1988) 70–77.

[10] G.A. Ibrahim, G.A. Vinnicombe, A hybrid method to analyses the performance of falling film absorbers, Int. J. Heat Mass Transfer 36 (1993) 1383–1390.

[11] JSME (Japan Society for Mech. Engrs.) Data Book, The Thermophysical Properties of Fluid, JSME, Tokyo, Japan, p. 208.

[12] A. Bakopoulos, Liquid-side controlled mass transfer in wetted-wall tube, Ger. Chem. Eng. 3 (1980) 241–252.

[13] A.P. Lamourelle, O.C. Sandall, Gas absorption into a turbulent liquid, Chem. Eng. Sci. 27 (1972) 1035–1043.

[14] J.H. Lienhard, in: A Heat Transfer Textbook, Prentice-Hall, New Jersey, 1981, pp. 399–400.

[15] S. Kamei, J. Oishi, J. Mem. Fac. Eng. Kyoto Univ. 18 (1956) 277–284.

[16] H. Hikita, K. Nakanishi, T. Nakaoka, J. Chem. Eng. Jpn. 23 (1959) 459–466.

[17] E.E. Emmert, R.L. Pigford, Chem. Eng. Prog. 50 (1954) 87–93.

[18] T. Nosoko, P.N. Yoshimura, T. Nagata, Characteristics of two-dimensional waves on a falling liquid film, Chem. Eng. Sci. 51 (1996) 725–732.

[19] P.N. Yoshimura, T. Nosoko, T. Nagata, Enhancement of mass transfer into a falling laminar liquid film by two-dimensional surface waves – some experimental observations and modeling, Chem. Eng. Sci. 51 (1996) 1231–1240.

[20] R.B. Bird, W.E. Stewart, E.N. Lightfoot, in: Transport Phenomena, Wiley, New York, 1960, pp. 668–672.

[21] G.A. Ratcliff, K.J. Reid, Mass transfer into spherical liquid films, Trans. Inst. Chem. Eng. 40 (1962) 69–74.

[22] J.F. Davidson, E.J. Cullen, D. Hanson, D. Roberts, The hold-up and liquid film coefficient of packed towers Part? Behavior of a string of spheres, Trans. Inst. Chem. Eng. 37 (1959) 122–130.